BJTA BRAZILIAN JOURNAL OF THERMAL ANALYSIS

Braz. J. Therm. Anal. Vol. 6 No. 1 DOI 10.18362/bjta.v6.i1

SYNTHESIS, THERMAL BEHAVIOUR AND CATALYTIC STUDY OF Ni-CHITOSAN IN TRANSESTERIFICATION REACTION USING SOYBEAN OIL

Caroline Gaglieri[1]; Flávio Junior Caires[1], Daniel J. Pamplona da Silva[2], Roberto Bertholdo[2], Roni Antônio Mendes*[2]

1 Faculdade de Ciências, UNES, Bauru, SP, Brazil
2 Instituto de Ciência e Tecnologia, UNIFAL-MG, Poços de Caldas, MG, Brazil
**carolinegaglieri@fc.unesp.br*

Acepted 15/08/2016
Published in 01/03/2017

Keywords

Chitosan
Nickel
Heterogeneous Catalyst
Biodiesel
Transesterification

DOI 10.18362/bjta.v6.i1.6

ABSTRACT

The biodiesel emerged as a substitute of standard diesel and could be considered a renewable and clean energy source. The transesterification reaction is considered the critical step in biodiesel production. The reaction between a short chain alcohol and chain triglycerides occurs in presence of a catalyst, which could be homogeneous or heterogeneous at reaction system. Trying solving the problems presented by homogeneous catalysis and finds viable applications conditions with heterogeneous catalysts, this work aimed to prepare and characterize a heterogeneous catalyst by chitosan with nickel (metallic complex) and then applies it in biodiesel production in laboratory scale. Simultaneous thermogravimetry and differential scanning calorimetry (TG-DSC) and Fourier Transform Infrared Spectroscopy (FTIR) to characterize the catalyst. To characterize the biodiesel were used Fourier Transform Infrared Spectroscopy and measurements of viscosity and density.

Introduction

The chitosan is the second most abundance polymer finds in the nature [1]. Its occurs could from alkaline deacetylations of chitin, which is finds exoskeleton of crustacean [1-3]. The units β- [1→ 4]-linked 2- acetamido-2-deoxy-D-glucopyranose and 2-amino-2-deoxy-D-glucopyranose constitute the polymer structure [2]. According Yong et al (2015) the polymer has to show a degree of deacetylation (DD) higher than 60% to be considered chitosan, a DD smaller indicates it is considered chitin. Between the applications of chitosan are the removal of heavy metals from industrial wastewater [3,4], drug delivery [5], and how catalyst in transesterification reaction [6-10]. In the last application, beside in its pure form, the chitosan has been tested how support to metallic materials [2].

This application is because the chitosan shows high affinity by metals due the presence of amines and hydroxyls groups in its structure, what induces specific properties in catalyst [2]. The sorption on metal on chitosan is controlled by the pH system. This interaction could be interpreted as an electrostatic attraction, or a formation of ion pairs and, the most common, metal chelation, depending of the pH used in synthesis [2]. In transesterification reaction the chitosan shows good results when applied how heterogeneous catalyst [6, 10]. This reaction occurs between triglyceride oil and a short-chain alcohol such as methanol or ethanol in presence of a catalyst [11]. The transesterification reaction is the critical step in biodiesel production [11, 12], which is considered as a sustainable energy source that takes the place of standard diesel [11], and could be realized under homogeneous or heterogeneous catalytic conditions [12-14]. Under homogeneous conditions some problems are observed, such as difficulty in separating the catalyst after end reaction [13, 14]. The research in heterogeneous catalyst has been increasing aim to solve some problems showed by the homogeneous catalysts, beside this, the use of heterogeneous catalyst provide a final product whit higher purity [13]. Trying to solve these problems and find viable applications conditions with heterogeneous catalysts, this work aimed to prepare and characterize a heterogeneous catalyst by chitosan with nickel (metallic complex) and then apply it in biodiesel production in laboratory scale.

Materials and Methods

The preparation of catalyst was by the precipitation method: aqueous solution (0.01 mol L^{-1}) of nickel chloride (Sigma Aldrich ≥ 98%) was prepared and then its pH was adjusted to 4.5. 1.0 gram of chitosan (Sigma Aldrich > 75% deacetylated) was added and the mixture was kept stirred for 2 hours. Thus after this time, the suspension was filtered vacuum, washed three times with distilled water, so the resulting was a green solid, that was stored in desiccator. The characterizations of chitosan and of the Ni-chitosan complex were obtained by simultaneous thermogravimetry and differential scanning calorimetry (TG-DSC) and Fourier Transform Infrared Spectroscopy (FTIR). TG-DSC curves were obtained using a Netzsch equipment, model STA 449 F3 Jupiter, using about 10 mg of sample, platinum crucibles of 30 μL, the purge gas were dry air and nitrogen with flow rate of 50 mL min^{-1}, and a temperature range of 30 -1000 ºC and a

Braz. J. Therm. Anal. Vol. 6 No. 1 DOI 10.18362/bjta.v6.i1

heating rate of 10 °C min^{-1} was adopted. The spectroscopic data were obtained using the Agilent Technologies equipment; model Agilent Cary 630 FTIR Spectrometer, operating in the range of 4000-650 cm^{-1} with ATR accessory and diamond crystal. The biodiesel was synthetized in homogeneous and heterogeneous conditions, ranging the catalyst and keeping up the reaction conditions, excepted by the time: 2 h to homogeneous catalysis and 72 h to heterogeneous catalysis. This variation was adopted because under same conditions, usually, the heterogeneous catalysis is slower than homogeneous catalysis to reach the equilibrium. The reagents used were soybean oil (commercial oil) and methanol (Merck ≥ 99.9 %) and the reactions conditions: molar ratio alcohol: vegetable oil was 6:1; catalyst: 1 w.t.% (mass fraction) relative to mass of soybean oil; and temperature at 60 ºC. NaOH, in solid state, was used as catalyst in homogeneous conditions, it was previously dissolved in methanol (1.65 mol L^{-1}) then the vegetable oil was added. Ni-chitosan was applied in heterogeneous system and chitosan was tested to verify if it is just a catalyst support or show any catalytic activity. The both compounds were added simultaneously with methanol and vegetable oil in reactional system. After ending transesterification reaction, the mixture was filtered with cotton then transferred to a separating funnel, thus was observed the separation in two phases, biodiesel (less dense) and glycerol (more dense). The superior phase was washed three times with distilled water at room temperature, and one more time with distilled water at 60 ºC. In the homogeneous catalysis, before the last wash, the system was washed with hydrochloric acid to neutralize the NaOH still present in solution. After all washes the solution pH was measurement. The drying of biodiesel was made in a kiln, at 80 ºC by 24 h. The product was stored in an amber bottle to prevent the photodegradation. All synthesis was made in triplicate. Biodiesel spectroscopy data were obtained by the same equipment and same conditions afore mentioned to catalyst characterization. The density and absolute viscosity of biodiesel were measured using a pycnometer and a digital viscometer of the Brookfield equipment, model Brookfield DV-I-Prime, using the SC4-18 spindle model at 12 rpm, respectively.

Results and Discussion

The TG-DSC curves of chitosan and Ni-chitosan complex in air and in nitrogen atmosphere are shown in Fig. 1 and Fig. 2 respectively. In air atmosphere the chitosan (Fig. 1.a) and Ni-chitosan complex (Fig.1.b) exhibited similar thermal behaviour: the first mass loss occurs in the range of 30 -141 ºC and were associated to dehydration of compounds as evidentiated by the endothermic peak in DSC curve. The content of water observed to chitosan was 11.69% and Ni-chitosan complex was 8.73%. The both compounds showed thermal stability until approximately 200 ºC, when the degradation of polymers started. This step occurs in two ranges: 202 - 367 and 367 - 601 ºC to chitosan; 199 - 369 and 369 - 595 ºC to Ni-chitosan and according with the DSC curves are associated to thermal degradation and oxidation of organic matter respectively. The final residues of Ni-chitosan (8.23%/ 6,47% de Ni) and of chitosan (3.64%) showed green and greyish white colour respectively. The first residue, probably, was NiO, while the second could be from process of production and purification of chitosan. To identify this residue, were realized two qualitative tests. The first test consisted in addition of dilute hydrochloric acid at residue. It was dissolved and any gas release was observed, excluding the carbonate presence. The second test was the flame test to identify the metal and associating the spectra observed (yellow) with the literature [15], the ion present could be the sodium. This information is consistent, considering the origin of chitosan. Then the residue of chitosan could be associated to Na_2O. The low adsorption of Ni, could be explained by the Hard Soft Acid Base (HSAB) theory: the OH and NH_2 groups are considered hard Lewis bases and borderline respectively [16]. Than some metals, considered soft Lewis acids, may shows unstable interaction with these groups, decreasing the sorption of these metals on chitosan [17].

The details of the decomposition steps for both compounds are shown in Table 1.

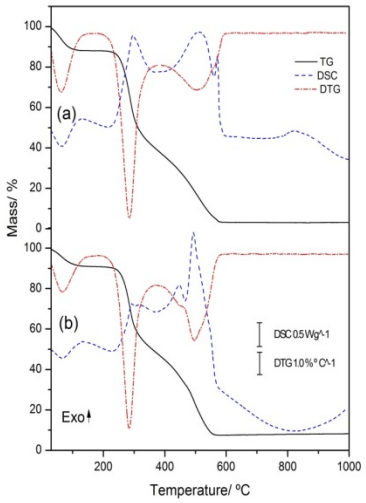

Figure 1 – TG-DSC curves in air atmosphere of *(a)* chitosan and *(b)* Ni-chitosan

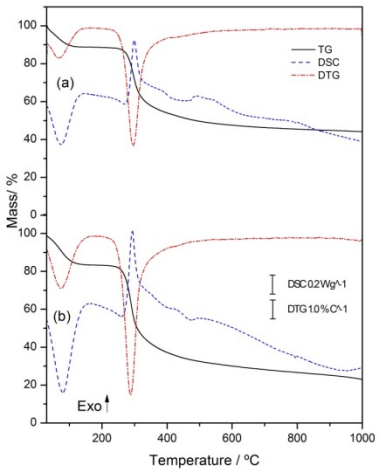

Figure 2 – TG-DSC curves and in nitrogen atmosphere *(c)* chitosan and *(d)* Ni-chitosan

The TG-DSC curves of chitosan and Ni-chitosan, obtaining under nitrogen atmosphere, are shown in Fig. 2.a and 2.b respectively. In TG-DSC curve of chitosan the first mass loss (11.08%), are associated to dehydration of samples according evidentiated by the DSC curves, and occurring between 30-160

Braz. J. Therm. Anal. Vol. 6 No. 1 **DOI 10.18362/bjta.v6.i1**

ºC approximately. The second mass loss of chitosan (34.99%) occurred in the range 212- 406 ºC, and was associated to thermal degradation of material, independent of atmosphere. The third mass loss (9.79%) was associated to degradation of material and is continue until the end of experiment, with a residue of 44.14% at 1000 ºC. The absence of oxidative atmosphere is the reason of this. The Ni-chitosan showed the similar thermal behavior: first mass loss (16.07 %) between 30-160 ºC, the second step (46.88%) and third step (14.02%) occurred between 197-404 and 404-1000 ºC, respectively. The value of chitosan residue (44.14%) is approximately the double of value of Ni-chitosan residue (23.03%). Associated with this, the degradation rate of chitosan, at second mass loss, were 6.25% min^{-1} or 0.67 $mgmin^{-1}$ and of the Ni-chitosan 8.43% min^{-1} or 0.88 mg min^{-1}, showing the nickel catalytic influence in the degradation step of organic matter. This result is in agreement with same works described in literature [18,19]. The detail of the decomposition steps under nitrogen atmosphere are shown in Table 1.

Table 1 - Thermal events of temperature (θ°C), mass loss (Δm) and temperature peak (T_P) observed in each TG-DSC curve steps of chitosan and Ni-chitosan complex under air and nitrogen atmosphere.

			1st step	2nd step	3rd step
Air	chitosan	θ °C	30-134	207.3-357.6	357.7-.597.1
		Δm/%	11.69	47.84	36.83
		T_P/°C	66.1 ↓	295.2↑	(514.5, 572.1) ↑
	Ni-chitosan	θ °C	30-141	205.2-369.1	369.1-584.6
		Δm/%	8.73	42.0	41.04
		T_P/°C	67.1 ↓	291.1↑	(447.0, 494.5) ↑
Nitrogen	chitosan	θ °C	30-160	212-406	406-1000
		Δm/%	11.08	34.99	9.79
		T_P/°C	74.3 ↓	299.0 ↑	(471.4-625)*
	Ni-chitosan	θ °C	30-160.2	196.7-404.1	404.1-1000
		Δm/%	16.07	46.88	14.02
		T_P/°C	79.9 ↓	293.2 ↑	(399.7-469.2)*

↑ = exo up; ↓ = endo down; exotherm *

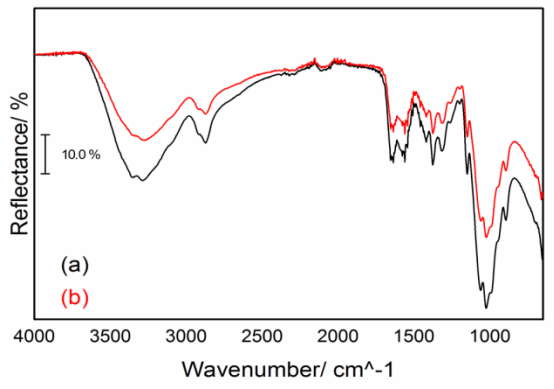

Figure 3 - FTIR spectra obtained from *(a)* chitosan and *(b)* Ni-chitosan

The FTIR spectrum obtained of chitosan are shown in Fig. 3a. The main bands are attributes to: O-H axial stretching between 3288-3362 cm^{-1}, at the same region are overlapping the N-H stretch of primary amines; C=O axial deformation of amide I between 1636 and 1648 cm^{-1}; symmetrical angular deformation of N-H between 1560- 1577; the bands at 1422 and 1062 cm^{-1} are associated to axial deformation of –CN present in amide and amine groups respectively [20] These results are in agreement with the results found by Santos et al (2003) and Sampo et al (2009) in their works [21,22]. The spectrum of Ni-chitosan, exhibit in Fig. 3.b, showed the same bands observed in chitosan spectrum. The most of bands could be overlapping, but the bands attributed to O-H and N-H groups were lightly displacement to 3262-3357 cm^{-1}. Beside this, these bands showed less intensity. This indicates that interaction of OH and NH_2 groups with metal.

To prove these interactions was applied the deconvolution method between 2400- 3850 cm^{-1}. The data were normalized and the Lorentz function was utilized to curves fitting. According with TG-DSC curves (Fig. 1) the both compounds were hydrates, so partially of bands disposed in this region are from water. To eliminate this interference, the samples of chitosan and Ni-chitosan were dried during 30 minutes; at temperatures of 135 and 150 ºC, respectively. These temperatures were determined by TG-DSC curves (Fig. 1). The curves fitting to chitosan and Ni-chitosan hydrate and dehydrate, and the values of area between baseline and the curve fitting to each peak are shown in Table 2 and Fig. 4., respectively.

Table 2 - Modules of the areas obtained by deconvolution method applied in the region 2400- 3850 cm^{-1} of IR spectra of chitosan and Ni-chitosan.

Compound	Hydrated				Dehydrated			
	Chitosan		Ni- Chitosan		Chitosan		Ni- Chitosan	
$R^2(10^{-2})$	99.8		99.7		99.5		99.1	
Peak	Area	Peak Center	Area	Peak Center	Area	Peak Center	Area	Peak Center
1	25.2	3485.1	16.4	3480.3	4.9	3492.7	1.9	3488.3
2	51.2	3379.0	29.6	3379.3	12.9	3385.8	5.5	3375.7
3	88.6	3253.4	54.2	3259.2	24.4	3259.0	9.4	3258.6
4	29.0	3102.8	29.8	3115.4	10.0	3104.7	9.0	3108.9
5	1.5	2926.3	1.0	2926.5	0.5	2933.9	0.2	2936.1
6	16.9	2873.1	11.6	2872.2	5.4	2877.1	3.6	2885.8
7	239.8	2737.8	177.9	2718.1	80.7	2697.9	42.2	2707.4

Braz. J. Therm. Anal. Vol. 6 No. 1 DOI 10.18362/bjta.v6.i1

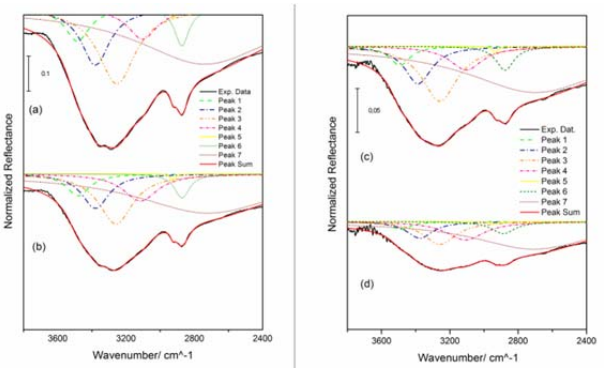

Figure 4 - Curves fitting by deconvolution method to *(a)* hydrate chitosan, *(b)* hydrate Ni-chitosan, *(c)* dehydrate chitosan and *(d)* dehydrate Ni-chitosan.

It is noted, except by peak 7 which curve fitting did not returned to baseline and must not be considering, that all center peak of hydrated samples are very close to the same variable of dehydrated sample. Then, to compare the variation of peaks, one of these was determined as reference. Dividing the peak from spectra hydrated chitosan by the same peak from spectra hydrated Ni-chitosan, and repeating this operation to dry compounds, the peak which less variation (3.8%) was the number 6. Then the other peaks was divided by this reference peak, the values obtained, shown in Table 3, to Ni-chitosan were different of chitosan; indicating that OH and NH_2 groups are involved in complexation with metal Ni.

Table 3 - Variation of area peaks (A_n) regarding the area of peak 6 (A_6)

Compound	Hydrated		Desydrated	
	Chitosan	Ni- chitosan	chitosan	Ni-chitosan
1	1.5	1.4	0.9	0.5
2	3.0	2.5	2.4	1.5
3	5.2	4.6	4.5	2.6
4	1.7	2.5	1.8	2.5
5	0.09	0.08	0.08	0.06
6	1.0	1.0	1.0	1.0
Peak	A_n/A_6			

Figure 5 - Catalyst deposited at botton after the end of heterogeneous reaction system.

After the end of each heterogeneous reaction, the catalysts, chitosan or Ni-chitosan, were deposited at bottom, showing be heterogeneous to reaction system (Fig. 5). Using the values measurement of density (ρ) and dynamic viscosity ($\boldsymbol{\mu}$), the kinematic viscosity ($\boldsymbol{\upsilon}$) were calculated. All these values are shown in Table 4.

Table 4 - Calculated kinematic viscosity ($\boldsymbol{\upsilon}$) with experimental data from transesterification reaction and soybean oil ($\boldsymbol{\nu = \mu/\rho}$).

Sample			ρ (kg m^{-3})	μ(cP)	υ (mm^2 s^{-1})
Soybean oil			914.5	47.5	51.9
homogenous		1	881.3	5.5	6.2
		2	882.5	5.2	5.9
		3	881.8	5.5	6.2
		average	881.8 ± 0.5	5.4 ± 0.1	6.1 ± 0.1
heterogeneous	chitosan	1	914.6	52.5	57,4
		2	914.7	51.7	56,5
		3	914.5	51.7	56,5
		average	914.6 ± 0.1	51.9 ± 0.4	56.8 ± 0.4
	Ni-chitosan	1	919.2	52.2	56.8
		2	914.7	52.2	57.1
		3	918.7	51.5	56.1
		average	917.5 ± 2.0	52.0 ± 0.3	56.6 ± 0.4

According to ANP to be considered as biodiesel, the product of transesterification need exhibit density and kinematic viscosity between 850-900 kg m^{-3} and 3-6 mm^2 s^{-1}, respectively [23]. The results of homogeneous catalyst are in agreement with this. In heterogeneous conditions the density obtained were higher than the limits stipulated by ANP, 1.6% (chitosan) and 1.9% (Ni-chitosan) and the values of kinematic viscosity are higher too. They are closer to value obtained to soybean oil, than the values of biodiesel; this indicates the possibility of low extension or non-occurrence of transesterification reaction under heterogeneous conditions.

The FTIR spectra of soybean oil, and the biodiesel obtained from homogeneous and heterogeneous conditions are shown in Fig. 6. Due the similarity of the products obtained under same catalytic conditions, just one spectrum of each catalyst are show now; the FTIR spectrum for the other products of transesterification could be viewed in supplementary material (Figures S1, S2 and S3).

Braz. J. Therm. Anal. Vol. 6 No. 1 DOI 10.18362/bjta.v6.i1

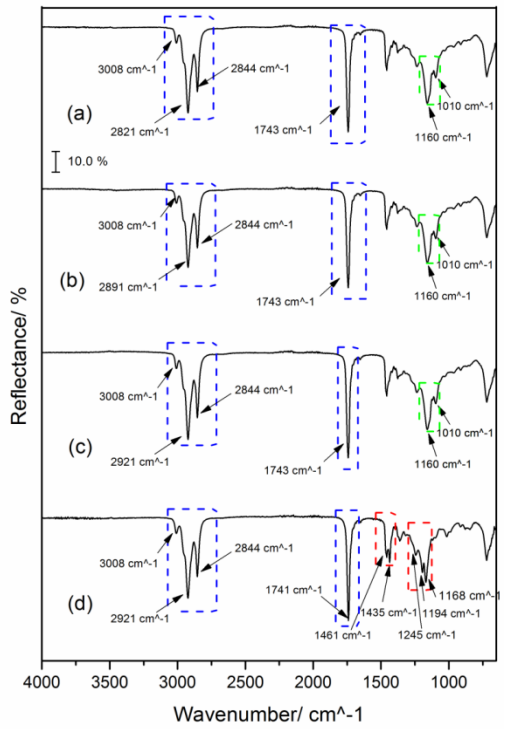

Figure 6 - Representative spectra of *(a)* soybean oil, and of the product obtained from transesterification reaction using the catalysts:*(b)* chitosan, *(c)*Ni-chitosan and *(d)* NaOH.

The FTIR spectrum of soybean oil (Figure 6.a) showed bands at 1101 and 1160 which are associated to the O−C stretch of O−CH_2C and to the C−C(=O)−O antisymmetric ester bond stretch, respectively, the both bands show the presence of try, di and monoglycerides presents at vegetable oil chain [24]. The band at 1743 cm^{-1} which is attributed to C=O vibrational stretching presents in triglyceride group [25]. The bands observed at 2844, 2921 and 3008 cm^{-1} are associated to C-H vibrational stretching [20]. Analysing the spectra of biodiesel from heterogeneous catalysis using the chitosan and Ni-chitosan complex as catalyst (Figure 6.b and 6.c respectively), were observed that they had very similarity to spectrum of soybean oil. Occurring practically the spectra overlap. This overlap didn't occur in spectrum of biodiesel obtained using NaOH as catalyst (Figure 6.d). Some bands are common to others spectra but, the bands at 1101 and 1160 cm^{-1} were not observed. In place of these, three bands are observed at 1168 cm^{-1}, 1194 cm^{-1} and 1245 cm^{-1}, which the first band is the most intense. This sequence of bands is feature of methyl esters of long chain fatty acids [20]. Further two bands are observed at 1435-1461 cm^{-1} which could be associated to antisymmetric stretch of O-CH_3 and the presence of FAME (fatty acid methyl esters) in product [24,25]. These presences of these bands indicate that under homogeneous conditions, there are FAME in final product of transesterification reaction. Any of these bands (1168, 1194, 1245, 1435 and 1461 cm^{-1}) were observed in product from heterogeneous conditions, but is not possible affirm the non-occur of transesterification reaction either its extend due to chemical groups with high similarity at reagent, reaction intermediate and final product.

Conclusion

How shows by TG-DSC curves approximately 5% of metal (Ni) was adsorbed on the surface of chitosan. The OH and NH_2 groups present in chitosan are involved in this interaction, how observed in deconvolution peak obtained in FTIR spectra. The metal nickel showed a catalytic effect in pyrolysis of organic matter, increasing the degradation rate of 0.67 to 0.88 mg min^{-1}. The catalyst proved be heterogeneous in this reaction system, however, the analyses of spectroscopy data and the values of density and viscosity obtained to transesterification product, concludes that the Ni-chitosan complex and chitosan showed low or no catalytic activity in production of biodiesel under the experimental conditions adopted.

References

[1] Mendes, A.A., de Castro, H. F., de Oliveira, P. C., Giordano, R. L. C. (2011). Aplicação da quitosana como suporte para imobilização de enzimas de interesse industrial. *Quimica Nova*, 34 (5), 831-840).

[2] Guibal, E (2005). *Heterogeneous catalysis on chitosan-based material: a review*. *Progress in polymer science*, 30, 71-109.

[3] Yong, S. K., Shrivastava, M., Srivastava P., Kunhikrishnan, A., Bolan, N. (2015). Environmental applications of chitosan and its derivates. *Reviews of Environmental Contamination Toxicology,* 233, 1-43.

[4] Fan, L., Luo, C., Sun, M., Li, M., Qiu, H. (2013). *Higly selective adsorption of lead ions by water-dispersible magnetic chitosan/graphene oxide composites*, 103, 523-529.

[5] Dunhaupt, S., Bernkop-Schnurch, A. (2012). Chitosan-based drug delivery systems. *European Journal of Pharmaceutics and Biopharmaceutics,* 81, 463-469.

[6] da Silva, R.B., Lima Neto, A. F., do Santos, L. S. S., Lima J. R. O., Chaves, M. H., dos Santos, J. R., de Lima, G. M., de Moura, E. M., de Moura, C. V. R. Catalysts of Cu (II) and Co (II) ions adsorbed in chitosan used in transesterification os foy bean and babassu oils- A new route for biodiesel syntheses. *Bioresource Thecnology,* 99, 6793-6798.

[7] ABREU, F.R., Alves, M.B., Macêdo, C.C.S., Zara, L.F., Suarez, P.A.Z. (2005).New multi-phase catalytic systems based on tin compounds active for vegetable oil transesterification reaction. *Journal of Molecular Catalysis*, 227, 263-267.

[8] Caetano, C.S., Caiado, M., Farinha, J., Fonseca, I.M., Ramos, A.M., Vital, J., Castanheiro, J.E. (2013). Esterification of free acids over chitosan with sulfonic acid groups. *Chemical Engineering Journal*, 230- 567-572.

[9] Fu, C., Hung, T., Su, C., Suryani, D., Wu, W., Dai, W., Yeh, Y. (2011). Immobilization of calcium oxide onto chitosan beads as a heterogeneous catalyst for biodiesel production. *Polymer International,* 60, 957-962.

Braz. J. Therm. Anal. Vol. 6 No. 1 DOI 10.18362/bjta.v6.i1

[10] ALMERINDO, G.I., Probst, L.F.D,Campos, C.E.M.C., Almeida, R.M., Meneghetti, S.M.P., Meneghetti, M.R., Claces, J., Farjado, H. (2011). Magnesium oxide prepared via metal-chitosan complexation method: Application as catalyst transesterification of soybean oil and catalyst deactivation studies. *Journal of Power Sources*, 196, 8057-8063.

[11] Knotche, G., Gerpen, J.V., Krahl, J., Ramos, L.P. (2006).*Manual do Biodiesel.* Tradução de Luiz Pereira Ramos. São Paulo: Edgard Blücher.

[12] Lôbo, I. P., Ferreira, S. L.C. (2009). Biodiesel: parâmetros de qualidade e métodos analíticos.*Química Nova*, 32(6), 1596-1608.

[13] Bart, J. C. J.; Palmeri, N.; Cavallaro, S. (2010). *Biodiesel Science and Technology: from soil to oil*. Boca Raton: CRC Press LLC.

[14] Pandey, A. (2009). *Handbook of plant-based biofuels*.Nova York: CRC Press.

[15] Vogel, A. I. (1981). *Química analítica qualitativa*. Traduzido por Antônio Gimeno. 5. ed. São Paulo: Mestre Jou.

[16] Pearson, R.G. (1963). Hard and soft acids and bases. *Journal of the American Chemical Society,* 85, 3533–3539.

[17] Yong, S. K., Shrivastava, M., Srivastava, P., Kunhikrishnan, A., Bolan, N. (2015). Environmental applications of chitosan and its derivatives. *Reviwes of Environmental Contamination and Toxicology*, 233, 1-43.

[18] Xing, S., Yuan, H. Qi, Y., Lv, P., Yuan, Z., Chen, Y. (2016) Characterization of the decomposition behaviours of catalytic pyrolysis of wood using copper and potassium over thermogravimetric and Py-GC/MS analysis.

[19] Miyazawa, T., Nishikawa, J., Kado, S., Kunimori, K., Tomishige, K. (2006). Catalytic performance of supported Ni catalyst in partial oxidation and steam reforming of tar derived from the pyrolysis of wood biomass. *Catalyst Today,* 115, 254-262.

[20] Silverstein, N, R. M., Webster, F. X., Kiemle, D. J. (2007).*Identificação espectrométrica de compostos orgânicos*. Tradução de Ricardo Bicca de Alencastro. Rio de Janeiro: LTC.

[21] dos Santos, J.E., Soares, J. P., Dockal, E. R., Campana Filho, S. P., Cavalheiro, E. T. G. (2003). Caracterização de quitosanas comerciais de diferentes origens. *Polímeros: Ciência e Tecnologia*, 13(4), 242-249.

[22] Sanpo, N., Ang, S.M., Cheang, P., Khor, K.A. (2009). Antibacterial Property of Cold Sprayed Chitosan-Cu/Al Coating.*Journal of thermal Spray Technology*, 18(4), 600-608.

[23] ANP.Constituição (2008).Lei nº 7, de 2008. *Resolução Anp Nº 7, de 19.3.2008 - Dou 20.3.2008.*

[24] Zhang, F., Adachi, D., Tamalampudi, S., Kondo, A., Tominaga, K. (2013). Real-time monitoring of the transesterification of soybean oil and methanol by Fourier-Transform infrared spectroscopy. *Energy Fuels*, 27, 5957- 5961.

[25] Natalello, A., Sasso, F., Secundo, F. (2013). Enzymatic transesterification monitored by an easy-to-use Fourier transform infrared spectroscopy method. *Biotechnology Journal*, 8, 133-138.